BUCKLING OF CYLINDRICAL PANELS BY A RITZ SCHEME

Lucas Nobumichi Yshii

Rafael Christovão Santana

Francisco Alex Correia Monteiro

Eliseu Lucena Neto

lucasyshii@gmail.com

rafael.feg@gmail.com

facm@ita.br

eliseu@ita.br

Instituto Tecnológico de Aeronáutica

Praça Marechal Eduardo Gomes, 50, 12228-900, São José dos Campos, SP, Brazil

Abstract. *A Ritz scheme is proposed for the linear buckling of circular cylindrical panels with stringers attached to the straight edges. Boundary conditions differ from the classical simply supported ones in the sense that the torsion resisted by the stringers is also taken into account. The Ritz bases are generated from an appropriate integration of the Legendre polynomials. Benchmark data verify the effectiveness of the formulation.*

Keywords: *Ritz method, Cylindrical panels, Buckling analysis*

1 INTRODUCTION

Circular cylindrical panels are important structural components in many engineering applications, such as aircraft fuselages, exteriors of rockets, submarine hulls, offshore platforms, and many others. The skin of a fuselage, for instance, can be thought of as an assembly of cylindrical panels supported by frames (circumferential stiffeners) and stringers (longitudinal stiffeners). Typically, these panels are the structural components most susceptible to buckling (Kollár & Dulácska, 1984; Buermann *et al.*, 2006).

The classical simply supported conditions, often assumed for design purposes, are represented by the requirement that the radial displacements and the bending moments be zero along the edges of an isolated panel, in addition to the constraint of null tangential displacements and normal in-plane stress resultants associated to the buckling deformation. Unlike the above-mentioned conditions, in this work the bending moments along the panel straight edges are not made zero but equal to the torsion resisted by the attached stringers. This will make these edges to be somewhere between simply supported and clamped. The linearized Donnell's equations, with prebuckling rotations neglected, are chosen to describe the panel buckling behavior (Brush & Almroth, 1975). The stringers are supposed to resist torsion in two ways: the first is denoted by Saint-Venant torsion, the second by warping torsion (Wunderlich & Pilkey, 2002). One contribution may be neglected as compared to the other for most practical cases. The warping torsion is usually negligible in bars with solid or thin-walled closed cross sections. Saint-Venant torsion, on the other hand, may be neglected in thin-walled open cross sections (Kollbrunner & Basler, 1969).

The Ritz method can pose low-grade convergence or numerical instability depending on the function basis selected (Baruh & Tadikonda, 1989; Oosterhout *et al.*, 1995) , no matter whether anisotropy is involved or not. For instance, the use of beam functions over constrains plates with free edges (Bassily & Dickinson, 1975; Dickinson & Di Blasio, 1986), and high-order polynomials can trigger numerical instabilities for being too much alike (Hjelmstad, 2005) or evaluated with round-off errors (Beslin & Nicolas, 1997). Anisotropic plates with simply supported edges are also over-constrained by beam functions (Nallim & Grossi, 2003; Gawandi *et al.*, 2008). The pursuit of a versatile Ritz basis to accurately predict the buckling solution has led the authors to identify the master numerical efficiency of the polynomial hierarchic set found in Bardel (1991). This polynomial set has demonstrated a high approximation capability even under severe anisotropy (Yshii *et al.*, 2016).

The exact solution for buckling of axially compressed cylindrical panels with all edges simply supported is easy to be found (Timoshenko & Gere, 1961; Reddy, 2004). Inclusion of the torsion resistance due to the stringers attached to the straight edges makes the problem complicated, for which an exact solution is difficult to be identified. An exact solution for the boundary-value problem which describes the linear buckling of axially compressed circular cylindrical panels with stringers attached to the straight edges is proposed by Lucena Neto *et al.* (2015, 2016). Such an investigation was motivated by the authors' need for benchmarks to test the accuracy of a fast tool to predict the skin buckling of reinforced cylindrical shells. Herein we present the first results of the developed analysis tool ALS (Analysis of Laminated Shells) which accuracy is preliminary verified by benchmark data.

2 RITZ EQUATIONS

Figure 1a depicts a circular cylindrical panel of radius R, length a, width b and thickness h, subjected to a uniform distributed axial compressive force p per unit length and referred to a set of orthogonal curvilinear coordinates xyz placed in the panel midsurface. The panel buckling is supposed to be described by the linearized Donnell's equations

$$\begin{aligned} u_{,xx} + \frac{1-\nu}{2} u_{,yy} + \frac{1+\nu}{2} v_{,xy} + \frac{\nu}{R} w_{,x} &= 0 \\ \frac{1+\nu}{2} u_{,xy} + \frac{1-\nu}{2} v_{,xx} + v_{,yy} + \frac{1}{R} w_{,y} &= 0 \\ \frac{A}{R}\left(\nu u_{,x} + v_{,y} + \frac{1}{R} w\right) + D\left(w_{,xxxx} + 2w_{,xxyy} + w_{,yyyy}\right) + p w_{,xx} &= 0 \end{aligned} \tag{1}$$

with prebuckling rotations neglected (Brush & Almroth, 1975). The quantities u, v and w are the midsurface displacements in the x, y and z directions, and a comma followed by x (or y) indicates differentiation with respect to x (or y). The panel has membrane and bending rigidities given by $A = Eh/(1-\nu^2)$ and $D = Eh^3/12(1-\nu^2)$, material with Young's modulus E and Poisson's ratio ν.

The solution of Eq (1) should satisfy prescribed values of

$$\begin{array}{lllll} N_x = 0 & v = 0 & w = 0 & M_x = 0 & : x = 0, a \\ u = 0 & N_y = 0 & w = 0 & M_y = \bar{M} & : y = 0, b \end{array} \tag{2}$$

where

$$\begin{aligned} N_x &= A\left(u_{,x} + \nu v_{,y} + \frac{\nu}{R} w\right) & M_x &= -D\left(w_{,xx} + \nu w_{,yy}\right) \\ N_y &= A\left(\nu u_{,x} + v_{,y} + \frac{1}{R} w\right) & M_y &= -D\left(\nu w_{,xx} + w_{,yy}\right). \end{aligned} \tag{3}$$

At buckling onset, the external moments

$$\bar{M}(x,0) = \left(G_s J_s w_{,xxy} - E_s \Gamma_s w_{,xxxxy}\right)\big|_{y=0} \qquad \bar{M}(x,b) = \left(-G_s J_s w_{,xxy} + E_s \Gamma_s w_{,xxxxy}\right)\big|_{y=b} \tag{4}$$

exerted by the stringers on the panel edges $y = 0, b$ prevent them from rotating freely. The stringers have torsional and warping constants given by J_s and Γ_s, material with Young's modulus E_s and shear modulus G_s, and are twisted by an amount $w_{,y}$. The first and second terms in $\bar{M}$ are associated with Saint-Venant and warping torsions, respectively.

Equation (1) and homogeneous form of the mechanical boundary conditions ($N_x = 0$ and $M_x = 0$ on $x = 0, a$; $N_y = 0$ and $M_y = 0$ on $y = 0, b$) can be stated as the stationary condition $\delta\Pi = 0$ of the potential energy

$$\Pi = \Pi_p(u, v, w) + \Pi_s(w) \tag{5}$$

with respect to u, v, w (Washizu, 1982). The potential energy of the shell panel is given by

$$\begin{aligned} \Pi_p = \frac{1}{2}\int_0^b \int_0^a \Bigg\{ & A\left[u_{,x}^2 + 2\nu u_{,x}\left(v_{,y} + \frac{w}{R}\right) + \left(v_{,y} + \frac{w}{R}\right)^2 + \frac{1-\nu}{2}\left(u_{,y} + v_{,x}\right)^2\right] \\ & + D\left[w_{,xx}^2 + 2\nu w_{,xx} w_{,yy} + w_{,yy}^2 + 2(1-\nu) w_{,xy}^2\right] - p w_{,x}^2 \Bigg\} dxdy \end{aligned} \tag{6}$$

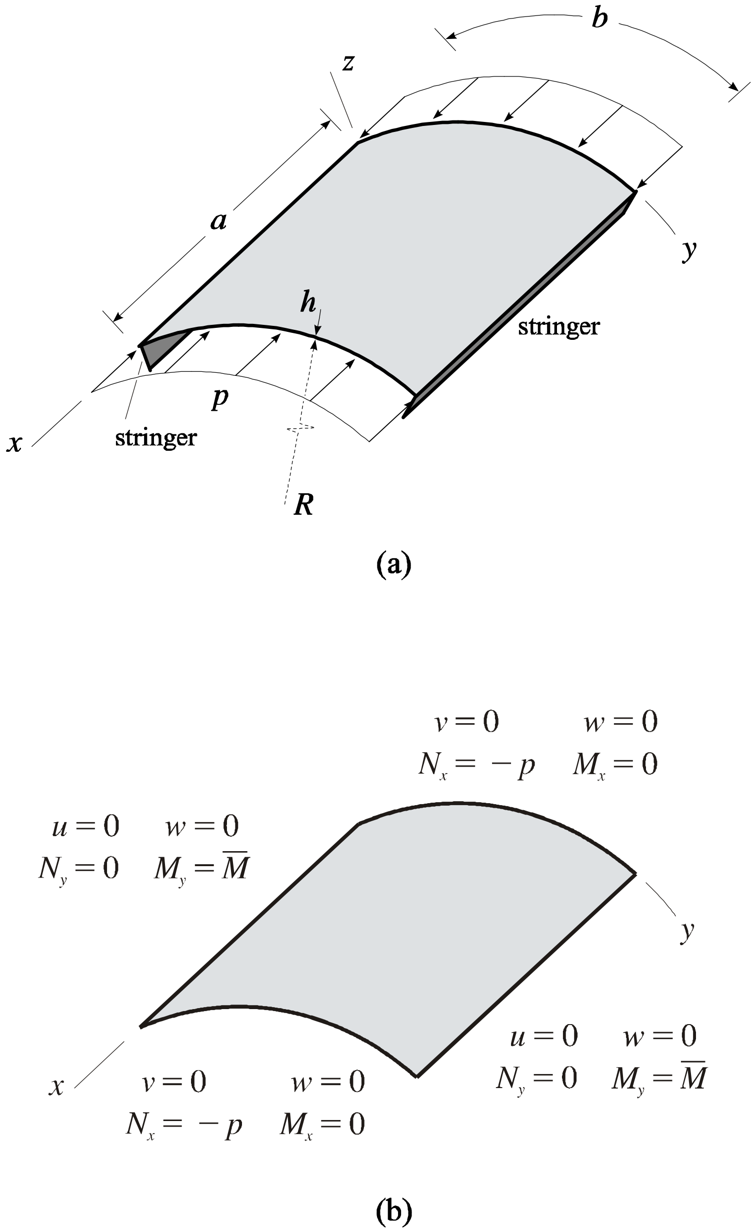

Figure 1: Cylindrical panel: (a) geometry and loading; (b) boundary conditions

whereas the potential energy of the stringers reads

$$\Pi_s = \frac{1}{2}\int_0^a \left[\left(G_s J_s w_{,xy}^2 + E_s \Gamma_s w_{,xxy}^2\right)\Big|_{y=0} + \left(G_s J_s w_{,xy}^2 + E_s \Gamma_s w_{,xxy}^2\right)\Big|_{y=b} \right] dx. \tag{7}$$

It is convenient to nondimensionalize the potential energy by adopting the coordinates $\xi = (2x - a)/a$ and $\eta = (2y - b)/b$ to obtain

$$\begin{aligned}\Pi_p = \frac{2}{ab}\int_{-1}^{1}\int_{-1}^{1} \Bigg\{ & A\left[\frac{b^2}{4}u_{,\xi}^2 + \frac{\nu ab}{2}u_{,\xi}\left(v_{,\eta} + \frac{bw}{2R}\right) + \frac{a^2}{4}\left(v_{,\eta} + \frac{bw}{2R}\right)^2 + \frac{1-\nu}{2}\left(\frac{a}{2}u_{,\eta} + \frac{b}{2}v_{,\xi}\right)^2\right] \\ & + D\left[\frac{b^2}{a^2}w_{,\xi\xi}^2 + 2\nu w_{,\xi\xi}w_{,\eta\eta} + \frac{a^2}{b^2}w_{,\eta\eta}^2 + 2(1-\nu)w_{,\xi\eta}^2\right] - p\frac{b^2}{4}w_{,\xi}^2\Bigg\} d\xi d\eta\end{aligned}$$

$$\Pi_s = \frac{2}{ab}\int_{-1}^{1}\left[\left(\frac{2G_sJ_s}{b}w_{,\xi\eta}^2 + \frac{8E_s\Gamma_s}{a^2b}w_{,\xi\xi\eta}^2\right)\Bigg|_{\eta=-1} + \left(\frac{2G_sJ_s}{b}w_{,\xi\eta}^2 + \frac{8E_s\Gamma_s}{a^2b}w_{,\xi\xi\eta}^2\right)\Bigg|_{\eta=1}\right] d\xi. \tag{8}$$

The solution of the buckling problem, which must satisfy exactly the geometric boundary conditions, is approximately sought by the Ritz method in the form

$$u(\xi,\eta) = \mathbf{u}^T\mathbf{U}(\xi,\eta) \qquad v(\xi,\eta) = \mathbf{v}^T\mathbf{V}(\xi,\eta) \qquad w(\xi,\eta) = \mathbf{w}^T\mathbf{W}(\xi,\eta). \tag{9}$$

The unknown coefficients are collected in vectors $\mathbf{u}$, $\mathbf{v}$, $\mathbf{w}$ while the Ritz basis functions are collected in vectors $\mathbf{U}$, $\mathbf{V}$, $\mathbf{W}$. Substitution of Eq. (9) into the potential energy Eq. (5) reduces the discrete buckling problem to the linear eigenvalue problem

$$(\mathbf{k}_c - p\mathbf{k}_g)\,\mathbf{d} = \mathbf{0} \qquad \mathbf{d}^T = \lfloor\; \mathbf{u}^T \quad \mathbf{v}^T \quad \mathbf{w}^T \;\rfloor \tag{10}$$

by means of $\delta\Pi = 0$. The panel buckling load is the lowest eigenvalue p. The constitutive stiffness matrix can be decomposed in the form

$$\mathbf{k}_c = \begin{bmatrix} \mathbf{k}^{uu} & \mathbf{k}^{uv} & \mathbf{k}^{uw} \\ & \mathbf{k}^{vv} & \mathbf{k}^{vw} \\ \text{sym.} & & \mathbf{k}^{ww} \end{bmatrix} \tag{11}$$

with

$$\begin{aligned}\mathbf{k}^{uu} &= A\left[\frac{b^2}{4}\boldsymbol{\Delta}_{uu}^{1100} + \frac{1-\nu}{2}\frac{a^2}{4}\boldsymbol{\Delta}_{uu}^{0011}\right] \qquad \mathbf{k}^{uv} = A\frac{ab}{2}\left[\nu\boldsymbol{\Delta}_{uv}^{1001} + \frac{1-\nu}{2}\boldsymbol{\Delta}_{uv}^{0110}\right] \\ \mathbf{k}^{vv} &= A\left[\frac{a^2}{4}\boldsymbol{\Delta}_{vv}^{0011} + \frac{1-\nu}{2}\frac{b^2}{4}\boldsymbol{\Delta}_{vv}^{1100}\right] \qquad \mathbf{k}^{vw} = A\frac{a^2b}{4R}\boldsymbol{\Delta}_{vw}^{0010} \qquad \mathbf{k}^{uw} = \nu A\frac{ab^2}{4R}\boldsymbol{\Delta}_{uw}^{1000} \\ \mathbf{k}^{ww} &= A\frac{a^2b^2}{16R^2}\boldsymbol{\Delta}_{ww}^{0000} + D\left[\frac{b^2}{a^2}\boldsymbol{\Delta}_{ww}^{2200} + \nu\left(\boldsymbol{\Delta}_{ww}^{2002} + \boldsymbol{\Delta}_{ww}^{0220}\right) + \frac{a^2}{b^2}\boldsymbol{\Delta}_{ww}^{0022} + 2(1-\nu)\boldsymbol{\Delta}_{ww}^{1111}\right] \\ &\quad + \frac{2G_sJ_s}{b}\left(\bar{\boldsymbol{\Delta}}_{-1}^{1111} + \bar{\boldsymbol{\Delta}}_{1}^{1111}\right) + \frac{8E_s\Gamma_s}{a^2b}\left(\bar{\boldsymbol{\Delta}}_{-1}^{2211} + \bar{\boldsymbol{\Delta}}_{1}^{2211}\right)\end{aligned} \tag{12}$$

where

$$\boldsymbol{\Delta}_{ab}^{pqrs} = \int_{-1}^{1}\int_{-1}^{1}\frac{\partial^{p+r}\mathbf{A}}{\partial\xi^p\partial\eta^r}\frac{\partial^{q+s}\mathbf{B}^T}{\partial\xi^q\partial\eta^s}d\xi d\eta \qquad \bar{\boldsymbol{\Delta}}_{a}^{pqrs} = \int_{-1}^{1}\left(\frac{\partial^{p+r}\mathbf{W}}{\partial\xi^p\partial\eta^r}\frac{\partial^{q+s}\mathbf{W}^T}{\partial\xi^q\partial\eta^s}\right)\Bigg|_{\eta=a} d\xi \tag{13}$$

and the geometric stiffness matrix $\mathbf{k}_g$ reads

$$\mathbf{k}_g = \begin{bmatrix} \mathbf{0} & \mathbf{0} & \mathbf{0} \\ & \mathbf{0} & \mathbf{0} \\ \text{sym.} & & \mathbf{k}^p \end{bmatrix} \qquad \mathbf{k}^p = \frac{b^2}{4}\mathbf{\Delta}_{ww}^{1100}. \tag{14}$$

The Ritz basis functions $\mathbf{U}$, $\mathbf{V}$, $\mathbf{W}$ are written in the separable form

$$\mathbf{U} = \begin{Bmatrix} X_{u1}(\xi)\,\mathbf{Y}_u \\ \vdots \\ X_{um}(\xi)\,\mathbf{Y}_u \end{Bmatrix} \quad \mathbf{V} = \begin{Bmatrix} X_{v1}(\xi)\,\mathbf{Y}_v \\ \vdots \\ X_{vm}(\xi)\,\mathbf{Y}_v \end{Bmatrix} \quad \mathbf{W} = \begin{Bmatrix} X_{w1}(\xi)\,\mathbf{Y}_w \\ \vdots \\ X_{wm}(\xi)\,\mathbf{Y}_w \end{Bmatrix}$$

$$\mathbf{Y}_u = \begin{Bmatrix} Y_{u1}(\eta) \\ \vdots \\ Y_{un}(\eta) \end{Bmatrix} \qquad \mathbf{Y}_v = \begin{Bmatrix} Y_{v1}(\eta) \\ \vdots \\ Y_{vn}(\eta) \end{Bmatrix} \qquad \mathbf{Y}_w = \begin{Bmatrix} Y_{w1}(\eta) \\ \vdots \\ Y_{wn}(\eta) \end{Bmatrix} \tag{15}$$

with m functions $X_{ui}(\xi)$, $X_{vi}(\xi)$, $X_{wi}(\xi)$ and n functions $Y_{ui}(\eta)$, $Y_{vi}(\eta)$, $Y_{wi}(\eta)$ in the ξ and η directions, respectively, to be selected from the polynomial set $\mathbf{F}_{\bar{B}}$ found in Bardell (1991), as summarized in the sequel.

Set of functions $\mathbf{F}_{\bar{B}}$

$$X_{u1}, X_{v1}, X_{w1} = \frac{1}{2} - \frac{3}{4}\xi + \frac{1}{4}\xi^3 \qquad X_{u2}, X_{v2}, X_{w2} = \frac{1}{8} - \frac{1}{8}\xi - \frac{1}{8}\xi^2 + \frac{1}{8}\xi^3$$

$$X_{u3}, X_{v3}, X_{w3} = \frac{1}{2} + \frac{3}{4}\xi - \frac{1}{4}\xi^3 \qquad X_{u4}, X_{v4}, X_{w4} = -\frac{1}{8} - \frac{1}{8}\xi + \frac{1}{8}\xi^2 + \frac{1}{8}\xi^3$$

$$X_{ui}, X_{vi}, X_{wi} = \sum_{n=0}^{(i-1)/2} \frac{(-1)^n}{2^n n!}\frac{(2i-2n-7)!!}{(i-2n-1)!}\xi^{i-2n-1} \qquad i = 5, 6, \ldots \tag{16}$$

Here $i!! = i\,(i-2)\ldots(2 \text{ or } 1)$, $0!! = (-1)!! = 1$, $(i-1)/2$ denotes its own integer part, and the functions $Y_{ui}(\eta)$, $Y_{vi}(\eta)$, $Y_{wi}(\eta)$ follow directly from $X_{ui}(\xi)$, $X_{vi}(\xi)$, $X_{wi}(\xi)$ on replacing ξ with η. The first four functions in $\mathbf{F}_{\bar{B}}$ correspond to the Hermite cubic polynomials and the remaing ones have been generated from Legendre polynomials by Zhu (1986) (see also Bardell (1991)) and possess both zero displacement and zero slope at each end. This features are significant since the higher modes contribute only to the internal displacement field, and all the classical geometric boundary conditions can be matched just by removing some of the first four basis functions. In the same manner as is done on finite element procedures, the boundary conditions may be introduced a posteriori into Eq. (10). Integrals in Eq. (13) are evaluated by symbolic computing to circumvent round-off errors and matrices $\mathbf{\Delta}_{ab}^{pqrs}$, $\bar{\mathbf{\Delta}}_{a}^{pqrs}$ are generated and stored in advance for $m = n = 104$. Such a procedure is only possible because the matrices are independent of panel geometry and material.

3 NUMERICAL RESULTS

We have written a code in MATLAB language to solve the linear eigenvalue problem given by Eq. (10) and conducted several tests adopting $m = n = 30$ as refinement level for approximations u, v, w in Eq. (9). All the analyzed panels have length $a = 500$ mm, thickness $h = 1$ mm, and material defined by $E = 72400$ N/mm^2, $\nu = 0.33$. Several values are attributed to the width b, radius R, and also to the stringer parameters J_s and Γ_s. The stringer material is given by $E_s = 71020$ N/mm^2, $G_s = 26700$ N/mm^2.

Table 1 summarizes the effect of the aspect ratio b/a and radius-to-thickness ratio R/h on the critical value of $\rho = p/p_{cl}$, where

$$p_{cl} = \frac{Eh^2}{R\sqrt{3\,(1-\nu^2)}} \tag{17}$$

identifies the minimum buckling load that a simply supported panel could ever achieve (Timoshenko & Gere, 1961), for panels under different stringer torsional J_s and warping Γ_s constants. The half-wave number, mode type (symmetric, antisymmetric) are indicated in parentheses. The pair ($J_s = 0$, $\Gamma_s = 0$) identifies panels under the classical simply supported boundary conditions. For such panels, the exact buckling load could also be reproduced by the expression

$$\rho = \min_{m,n} \left[\frac{Rh}{4\sqrt{3\,(1-\nu^2)}} \frac{\pi^2}{m^2 a^2} \left(m^2 + \frac{n^2 a^2}{b^2} \right)^2 + \frac{\sqrt{3\,(1-\nu^2)}}{Rh} \frac{m^2 a^2}{\pi^2} \left(m^2 + \frac{n^2 a^2}{b^2} \right)^{-2} \right] \tag{18}$$

in which the integers m and n stand for the numbers of longitudinal and circumferential half-waves of the buckling modes. The value $\rho = 1$ represents the minimum value that a simply supported panel could ever achieve by the adopted linear buckling analysis. The buckling load for ($R/h = 500$, $b/a = 0.8$), ($R/h = 500$, $b/a = 1.4$) and ($R/h = 1000$, $b/a = 1.0$) have been rounded to five decimal places for representation purposes, being indeed slightly greater than unity.

Pairs ($J_s \neq 0$, $\Gamma_s \neq 0$) identify panels with stringers attached to the straight edges. For such panels, the exact buckling loads presented in Table 1 may be considerably higher than those predicted by neglecting the stringer contribution. With ($J_s = 0$, $\Gamma_s = 0$), the buckling load is underpredicted mainly for narrower (small b/a) and shallower (large R/h) panels. For instance, a panel with $b/a = 0.2$ and $R/h = 1500$ attached to stringers with ($J_s = 96$ mm^4, $\Gamma_s = 36370$ mm^6) buckles at a load somewhat 51% higher than that load obtained by neglecting the stringer contribution. Surprisingly, all the obtained results coincide with the benchmark data presented by Lucena Neto *et al.* (2016) considering five decimal places, except for the panel with $b/a = 0.2$ and $R/h = 1000$ attached to stringers with ($J_s = 96$ mm^4, $\Gamma_s = 36370$ mm^6) for which the predicted buckling load is 0,00073% higher than the exact one. These examples illustrate the high approximation capability of the hierarchic polynomial set Eq. (16).

For comparison purpose, linear buckling predictions have also been conducted with the finite element modeling (FEM) package NASTRAN whose results are shown in Table 2. It can be seen that the FEM results are consistently different than the exact ones previously reported. This anomaly can be explained by the fact that the rigorous prebuckling solutions computed by NASTRAN differ from the membrane prebuckled shape assumed in the classical buckling theory. The lack of a rigorous prebuckled shape in classical buckling theory leads to some inaccuracies in calculated axial compression buckling loads. The results obtained by the proposed Ritz scheme are in total agreement with the classical buckling theory whilst the difference in the FEM predictions gets progressively higher for narrow panels.

4 CONCLUSIONS

A Ritz scheme based on a set of modified Legendre functions has been presented for buckling analysis of isotropic cylindrical panels under axial compression with stringers attached to the straight edges. Accurate and stable solutions according to the classical buckling theory have been obtained, validating the effectiveness of the formulation under the membrane prebuckled assumption.

REFERENCES

Bardell, N. S., 1991. Free vibration analysis of a flat plate using the hierarchical finite element method. *Journal of Sound and Vibration*, vol. 151, n. 2, pp. 263-289.

Baruh, H., & Tadikonda, S. S. K., 1989, Another look at admissible functions, vol. 132, n. 1, *Journal of Sound and Vibration*, pp. 73-87.

Bassily, S. F., & Dickinson, S. M., 1975. On the use of beam functions for problems of plates involving free edges. *Journal of Applied Mechanics*, vol. 42, n. 4, pp. 858-864.

Beslin, O., & Nicolas, J., 1997. A hierarchical functions set for predicting very high-order plate bending modes with any boundary conditions. *Journal of Sound and Vibration*, vol. 202, n. 5, pp. 633-655.

Brush, D. O., & Almroth, B. O., 1975. *Buckling of Bars, Plates, and Shells*. McGraw-Hill, New York.

Buermann, P., Rolfes, R., Tessmer, J., & Schagerl, M., 2006. A semi-analytical model for local post-buckling analysis of stringer- and frame-stiffened cylindrical panels. *Thin-Walled Structures*, vol. 44, n. 1, pp. 102-114.

Dickinson, S. M., & Di Blasio, A., 1986. On the use of orthogonal polynomials in the Rayleigh-Ritz method for the study of the flexural vibration and buckling of isotropic and orthotropic rectangular plates. *Journal of Sound and Vibration*, vol. 108, n. 1, pp. 51-62.

Gawandi, A., Whitney, J. M., & Brockman, R. A., 2008. Natural boundary conditions in the bending of anisotropic laminated plates. *Composite Structures*, vol. 82, n. 2, pp. 201-208.

Hjelmstad, K. D., 2005. *Fundamentals of Structural Mechanics*. Springer, New York.

Kollár, L., & Dulácska, E., 1984. *Buckling of Shells for Engineers*. Wiley, Chichester.

Kollbrunner, C. F., & Basler, K., 1969, *Torsion in Structures*. Springer, Berlin.

Lucena Neto, E., Monteiro, F. A. C., & Soares, P. T. M. L., 2015. Rigorous Solution for Axially-Compressed Cylindrical Panels. In *XXXVI Iberian Latin-American Congress on Computational Methods in Engineering (CILAMCE-2015)*, Rio de Janeiro, Brazil.

Lucena Neto, E., Monteiro, F. A. C., & Soares, P. T. M. L., 2016. Exact solution for buckling of axially compressed cylindrical panels with stringers attached to the straight edges. *Journal of Engineering Mechanics*, vol. 142, n. 6, pp. 04016028-1-04016028-10.

Nallim, L. G., & Grossi, R. O., 2003. On the use of orthogonal polynomials in the study of anisotropic plates. *Journal of Sound and Vibration*, vol. 264, n. 5, pp. 1201-1207.

Reddy, J. N., 2004. *Mechanics of Laminated Composite Plates and Shells: Theory and Analysis*. CRC Press, Boca Raton.

Oosterhout, G. M., Hoogt, P. J. M., & Spiering, R. M. E. J., 1995, Accurate calculation methods for natural frequencies of plates with special attention to the higher modes. *Journal of Sound and Vibration*, vol. 183, n. 1, pp. 33-47.

Timoshenko, S. P., & Gere, J. M., 1961, *Theory of Elastic Stability*, 2nd edn. McGraw-Hill, New York.

Washizu, K., 1982. *Variational Methods in Elasticity and Plasticity*, 3rd edn. Pergamon Press, Oxford.

Wunderlich, W., & Pilkey, W. D., 2002. *Mechanics of Structures: Variational and Computational Methods*, 2nd edn. CRC Press, Boca Raton.

Yshii, L. N, Santana, R. C., Monteiro, F. A. C., & Lucena Neto, E., 2016. Buckling of Anisotropic Plates by the Ritz Method. In *XXXVII Iberian Latin-American Congress on Computational Methods in Engineering (CILAMCE-2016)*, Brasília, Brazil.

Zhu, D. C., 1986. Development of hierarchical finite element methods at BIAA, vol. 1. In *Proceedings of the International Conference on Computational Mechanics*, Tokyo, Japan.

Table 1: Effect of the aspect ratio b/a and radius-to-thickness ratio R/h on the critical value of ρ for panels under several pairs (J_s, Γ_s) of stringer constants

		R/h		
(J_s, Γ_s)	b/a	500	1000	1500
(0, 0)	0.2	1.00171 (10, s)	1.01779 (5, s)	1.18156 (5, s)
	0.4	1.00152 (12, s)	1.00256 (8, s)	1.00122 (1, s)
	0.6	1.00004 (12, a)	1.00102 (9, s)	1.00004 (7, s)
	0.8	1.00000 (8, s)	1.00012 (2, s)	1.00026 (4, s)
	1.0	1.00018 (12, s)	1.00000 (9, s)	1.00017 (6, s)
	1.2	1.00004 (12, a)	1.00001 (9, s)	1.00004 (7, a)
	1.4	1.00000 (6, s)	1.00001 (3, a)	1.00018 (6, a)
(96, 36370)	0.2	1.08832 (11, s)	1.37402 (8, s)	1.78693 (8, s)
	0.4	1.00728 (12, s)	1.02491 (8, s)	1.05119 (7, s)
	0.6	1.00280 (13, s)	1.00579 (9, s)	1.00995 (7, s)
	0.8	1.00125 (13, s)	1.00178 (9, s)	1.00481 (7, s)
	1.0	1.00074 (13, s)	1.00071 (9, s)	1.00427 (7, s)
	1.2	1.00052 (13, s)	1.00036 (9, s)	1.00360 (7, a)
	1.4	1.00041 (13, s)	1.00023 (9, s)	1.00246 (7, a)
(12372, 1582)	0.2	1.08939 (11, s)	1.38442 (8, s)	1.80290 (8, s)
	0.4	1.00731 (12, s)	1.02539 (8, s)	1.05271 (7, s)
	0.6	1.00281 (13, s)	1.00585 (9, s)	1.01021 (7, s)
	0.8	1.00125 (13, s)	1.00180 (9, s)	1.00487 (7, s)
	1.0	1.00074 (13, s)	1.00072 (9, s)	1.00428 (7, s)
	1.2	1.00052 (13, s)	1.00036 (9, s)	1.00367 (7, a)
	1.4	1.00041 (13, s)	1.00023 (9, s)	1.00248 (7, a)

Table 2: NASTRAN predictions of ρ for panels under several pairs $(J_s,\ \Gamma_s)$ of stringer constants

		R/h		
$(J_s,\ \Gamma_s)$	b/a	500	1000	1500
(0, 0)	0.2	2.36669	1.46115	1.25150
	0.4	1.16074	1.04235	0.96957
	0.6	0.94320	0.87710	0.85190
	0.8	0.88991	0.87279	0.88461
	1.0	0.90010	0.93476	0.93867
	1.2	0.94611	0.93996	0.91947
	1.4	0.94957	0.92689	0.91865
(96, 36370)	0.2	4.38447	2.95722	2.28755
	0.4	1.02473	1.27507	1.14378
	0.6	0.09580	0.89428	0.86218
	0.8	0.89480	0.87204	0.87180
	1.0	0.90122	0.92607	0.93772
	1.2	0.94526	0.94887	0.92747
	1.4	0.95635	0.93366	0.92206
(12372, 1582)	0.2	5.07497	3.01325	2.29228
	0.4	1.78829	1.40618	1.20798
	0.6	1.05307	0.91075	0.86478
	0.8	0.91195	0.86754	0.86502
	1.0	1.04734	0.91410	0.93292
	1.2	0.94205	0.94804	0.92746
	1.4	0.96968	0.93633	0.92069